Theory of heat dissipation in molecular electronics

A. Pecchia, G. Romano, and A. Di Carlo
Department of Electronics Engineering, University of Rome "Tor Vergata," Via del Politecnico 1, 00133 Roma, Italy
(Received 11 August 2006; revised manuscript received 3 November 2006; published 2 January 2007)

In this paper we discuss various aspects of energy dissipation and heating of molecular junctions under bias. First-principles calculations based on density functional and nonequilibrium Green's functions are used to compute the power emitted in a molecule due to scattering with localized vibrations. In this context, we present a perturbation scheme in the electron-phonon coupling, that is found numerically reliable for the computation of the emitted power, because intrinsically it is current conserving. The balance between the rate of phonons emitted and dissipated into the contacts allows the computation of the steady-state distribution of phonon quanta localized in the junction, from which we extract the local temperature reached by the molecule. The model includes a microscopic approach for the computation of the phonon decay rate, accounting for the dynamical coupling between the vibrational modes localized on the molecule and the contact phonons. The method is applied to the discussion of several limiting conditions and trends, depending on electron-phonon coupling, incoherent transmission and phonon dissipation rate using both analytical results and numerical calculations.

DOI: 10.1103/PhysRevB.75.035401 PACS number(s): 73.63.Rt, 72.10.−d, 72.15.Jf

I. INTRODUCTION

Whether molecular electronics will be a technological reality in some future it will critically depend on the stability of the compounds under bias conditions. Current-induced forces and local heating effects are relevant parameters to be evaluated in order to assess the feasibility of such technology. Noticeably current-induced local heating in a molecular junction made of octane dithiol has been recently measured for the first time.[1] On the other hand, models and theories has been developed in recent years[2–6] to account for heat dissipation in nanojunctions. Most models include electron-vibration coupling and phonon release in molecular bridges and account for phonon dissipation into the heat reservoirs with some phenomenological parameter. In this research electron-vibration couplings are calculated from first principles and we show that heating effects in molecular junctions can be relevant, particularly when molecular resonances are hit.

Several aspects of power dissipation in a molecular junction are discussed. We start presenting some details of our density functional theory (DFT) scheme used to compute structural properties of the junctions, electronic states, and vibrational frequencies. In Sec. III we introduce the rate equation used to compute the steady state number of quanta in the vibrational degrees of freedom of the molecule, including the rate of phonon emitted and absorbed by the electron-phonon coupling as well as the rate of phonon dissipated into the bath. Within the same section we present the numerical strategies used to make the self-consistent computation of the nonequilibrium phonon population feasible. Our scheme guarantees current conservation and a correct calculation of the dissipated power and rate of phonon emission in the nanojunction even to first order of perturbation theory. Analytical results of local temperature vs bias are discussed in Sec. IV for the limiting case of energy-independent tunneling and density of states. In Sec. V the effect of a tunneling resonance and tunneling-assisted phonon emission is analyzed, showing that when molecular resonances are hit incoherent current can sharply increase, leading to a step in the local heating process. We conclude with a numerical application of the model to a styrene molecule bonded to a Si substrate via direct Si-C bonds in a scanning tunnel microscope (STM) geometry. In this calculation, electronic states, vibrational modes, electron-vibron coupling, and phonon damping to the reservoirs are computed from first principles. The application outlines the importance of considering the complete energy dependent transmission and shows the combined effect of tunneling resonances with electron-phonon coupling strengths in the determination of heat dissipation in molecular junctions.

II. THEORY

The electronic states of the contact-molecule-contact system are described via a local basis density functional scheme, where appropriate approximations are considered in order to make the approach efficient for a large number of atoms.[7–9] These include the use of an optimized minimal basis set and the neglect of three-center integrals. Both the electronic and the repulsive potential, is expressed as a superposition of atomic pair-potentials, obtained from *ab initio* DFT reference calculations[9] allowing extensive use of look-up tables. The whole method has been extended to nonequilibrium quantum transport calculations[10,11] self-consistent in the atomic charge density.

This method has proved to be successful in computing structural and electronic properties of various systems and also gives a good accuracy in the calculation of vibrational frequencies.[12,13]

Molecular vibrations and electron-vibron couplings are treated in the usual way,[14–17] after decoupling the Hamiltonian as a superposition of independent one-dimensional oscillators corresponding to the normal modes of vibrations, labeled by q. The harmonic oscillators can be quantized following the usual prescriptions, by making use of the standard

relationships between the position operator and the creation/annihilation field operators, a_q^+ and a_q. The result is a term in the Hamiltonian describing the electron-phonon coupling,

$$H_{el\text{-}ph} = \sum_{q,\mu,\nu} \gamma_{\mu\nu}^q c_\mu^+ c_\nu [a_q^+ + a_q], \tag{1}$$

where c_μ^+ and c_ν are, respectively, the creation and annihilation operators of one electron in the atomic basis and

$$\gamma_{\mu\nu}^\alpha = \sqrt{\frac{\hbar}{2\omega_q M_q}} \sum_\alpha \left[\frac{\partial H_{\mu\nu}}{\partial R_\alpha} - \sum_{\sigma,\lambda} \frac{\partial S_{\mu\sigma}}{\partial R_\alpha} S_{\sigma\lambda}^{-1} H_{\lambda\nu} - \sum_{\sigma,\lambda} H_{\mu\lambda} S_{\lambda\sigma}^{-1} \frac{\partial S_{\sigma\nu}}{\partial R_\alpha} \right] \mathbf{e}_\alpha^q, \tag{2}$$

are the electron-phonon coupling matrices. M_q are the atomic masses, ω_q the mode frequencies, and $\mathbf{e}_\alpha^q$ are the normalized atomic displacements for each mode. The nonorthogonality of the atomic basis set is reflected by the presence of the overlap matrix, $S_{\mu\nu}$, and its derivative with respect to the ionic positions, R_α.

Therefore, the ionic vibrations of a molecular wire can be described as a class of boson particles, here referred to as *phonons*. While crossing the system, electrons interact with the molecular ionic vibrations from which they can be inelastically scattered.

The electron-phonon interaction is treated within perturbation theory of the nonequilibrium Green's function formalism and the current through the junction is computed using the Meir-Wingreen formula (Ref. 18),

$$I = \frac{2e}{h} \int_{-\infty}^{+\infty} \mathrm{Tr}[\Sigma_L^<(\omega) G^>(\omega) - \Sigma_L^>(\omega) G^<(\omega)] d\omega, \tag{3}$$

where $\Sigma_L^{<(>)}$ represents the in-scattering of electrons (holes) through the *left* contact of the device, while $G^{<(>)}$ is the electron (hole) correlation function, obtained from the kinetic equations (Refs. 19 and 20),

$$G^{<(>)}(\omega) = G^r(\omega) \Sigma^{<(>)}(\omega) G^a(\omega), \tag{4}$$

and $G^{r(a)}$ are the retarded (advanced) Green's functions given by the usual expressions,

$$G^{r(a)}(\omega) = [\omega S - H - \Sigma^{r(a)}]^{-1}. \tag{5}$$

The current expressed by Eq. (3) contains both a coherent and a incoherent component, since the *lesser* and *greater* self-energies (SE) are given by the sum of three terms,

$$\Sigma^{<(>)}(\omega) = \Sigma_L^{<(>)}(\omega) + \Sigma_R^{<(>)}(\omega) + \Sigma_{ph}^{<(>)}(\omega). \tag{6}$$

The first two contributions come from the contacts and the third term is related to the scattering processes within the molecule, caused by electron-phonon interactions. Such decoupling is valid within the noncrossing approximation (NCA) that we took care to fulfill by physically separating the molecular subunit, free to move, from the contacts, where the atoms are assumed fixed. Such separation was obtained with three layers of atoms representing the metal surfaces which have been treated as to be part of the extended molecule. Because of the short range of the atomic orbital interactions and since the surface atoms do not move, such three layers ensure that the contact and electron-phonon self-energies act on orthogonal subspaces of the Hamiltonian matrix. This argument is valid within the other approximations used, such as the DFT-LDA (local density approximation) local orbital formulation of the single-electron Hamiltonian.

The electron-phonon self-energy can be evaluated with diagrammatic techniques. The self-consistent Born approximation (SCBA) is expressed by

$$\Sigma_{ph}^{<(>)}(\omega) = i \sum_q \int_{-\infty}^{+\infty} \frac{d\omega'}{2\pi} \gamma_q G^{<(>)}(\omega - \omega') \gamma_q D_q^{<(>)}(\omega'), \tag{7}$$

where $D_q^{<(>)}$ are the correlation functions related to the vibrational modes,

$$D_{0,q}^<(\omega) = -2\pi i [(N_q + 1)\delta(\omega + \omega_q) + N_q \delta(\omega - \omega_q)],$$

$$D_{0,q}^>(\omega) = -2\pi i [(N_q + 1)\delta(\omega - \omega_q) + N_q \delta(\omega + \omega_q)]. \tag{8}$$

assumed as Einstein oscillators, i.e., the vibron lifetimes are neglected in the electron-phonon calculation. Inserting (8) into (7) it is possible to derive an explicit form for the electron-phonon self-energy,

$$\Sigma_{ph}^< = \sum_q N_q \gamma_q G^<(E - \omega_q) \gamma_q + (N_q + 1) \gamma_q G^<(E + \omega_q) \gamma_q,$$

$$\Sigma_{ph}^> = \sum_q N_q \gamma_q G^>(E + \omega_q) \gamma_q + (N_q + 1) \gamma_q G^>(E - \omega_q) \gamma_q. \tag{9}$$

The self-consistency in Eq. (7) is implied by the use of a renormalized Green's function, $G^<$, whereas the first order Born approximation is obtained when the unrenormalized (zeroth order) Green's function is used to evaluate the electron-phonon self-energy. Using the relationship $\mathrm{Im}\{\Sigma_{ph}^r\} = 1/2(\Sigma_{ph}^> - \Sigma_{ph}^<)$ it is possible to compute Σ_{ph}^r that modifies the electron propagator in (5). Since we are mainly interested in the electron lifetime and we restrict to weak electron-phonon coupling, the real part of Σ_{ph}^r, responsible for a polaronic shift, is neglected. Consistently, we also neglect the first order Hartree diagram, which gives a contribution to the real part only.

III. SELF-CONSISTENT PHONON POPULATION

The key concept discussed in this paper is the power released in the system and the nonequilibrium local temperature reached by the molecular junction under bias. For this purpose a semiclassical approach has been followed by setting a simple rate equation (Ref. 5),

$$\frac{dN_q}{dt} = R_q - J_q[N_q - n_q(T_0)], \tag{10}$$

balancing the rate, R_q, of quanta emitted in the molecular mode q, with the decay rate, J_q, of the same vibrational mode

into the bath. The former contains the net emission of phonons into the molecule due to the electron-vibration coupling. The latter tends to restore the phonons to the equilibrium Bose-Einstein distribution, $n_q(T_0)$, characterized by the contact temperature, T_0. At steady state the phonon distribution on the molecule is given by $N_q=n_q(T_0)+R_q/J_q$. The present treatment neglects intramolecular decays due to anharmonic and contact mediated couplings between the modes. These terms can be included within a master equation approach coupling different modes. In the limit of very fast dynamics, quantum corrections should be taken into account by solving a dynamical (Keldysh) equation similar to (4) also for the phonon propagator.[21] Phonons, however, have relaxation times usually longer than the tunneling time, therefore the rate equation is sufficiently accurate for the purposes of the present analysis.

A. Rate of phonon dissipation

A crucial parameter for the computation of the molecular heating is the rate of phonon dissipation into the reservoirs, J_q. This is by no means a simple quantity to be predicted from first-principles calculations, since a large number of different mechanisms participate in phonon relaxations. For this reason J_q can be regarded in many cases as a fitting parameter of the model. Nonetheless an insight into a quantitative prediction of J_q is given in this work by considering the elastic coupling of the molecular modes with the contact vibrations. The calculation is performed by computing the Hessian (dynamical matrix) of the whole contact-molecule-contact device and by partitioning such system like it is done for the electron Hamiltonian, namely into molecule and contacts. A Green's function is then built for the vibration eigensystem,

$$\sum_j H_{ij}e_j^q = \sum_j M_{ij}e_j^q\omega_q^2, \tag{11}$$

using an open boundary condition on the bulk side of the contact leads. In Eq. (11), H_{ij} is the Hessian matrix, e_j^q are the normal modes of vibration, M_{ij} is the mass matrix, and ω_q are the mode frequencies. This formulation allows one to compute a self-energy for the vibron propagator, whose imaginary part is used to extract the vibron lifetime.

This treatment is essentially a Fermi golden rule including first-order one phonon to one phonon decay processes, but obviously neglects a large number of other mechanisms that may take place when the direct decay is forbidden. High frequency modes, characteristic of molecular vibrations, generally lay well beyond the vibrational bandwidth of the bulk reservoirs and cannot decay other than via one-to-many phonon channels.[22,23] Some of these effects can be taken into account introducing effective phonon densities for the contact modes.[24] This, for instance, allows the correct prediction of the temperature dependence of many-phonons decay rates. However, quantitative predictions of one-to-many phonons decay rates require the calculation of coupling constants related to anharmonic potentials, not explicitly treated in this work. Other decay mechanisms may also be represented by vibrational coupling with the surrounding molecules (and generally depends on the environment) or with multistep processes, first involving relaxations to lower energy modes via anharmonic couplings. Radiative decays may also play an important role. An accurate analysis of the subject is beyond the scope of this work and will be presented elsewhere.[25]

It is important to stress that damping directly related to electron-phonon coupling, such as the relevant decay via creation of electron-hole pairs is included in our formalism within R_q, as discussed in Appendix B.

As a result of the present simplified treatment, the phonon decay rate is fast ($\sim 10^{10}$–10^{12} Hz) for the energy modes lying within the contact bandwidth and sharply decreases beyond, reaching very small values. We return on this point in Sec. VI, in connection to an explicit calculation of such rates.

B. Rate of phonon emission

In order to calculate R_q, first we introduce the net power emitted into the junction, which is given by the net rate of energy transferred to the molecule and that can be calculated using (Ref. 26)

$$W = \frac{2}{h}\int_{-\infty}^{+\infty} \omega \mathrm{Tr}[\Sigma_{ph}^{<}(\omega)G^{>}(\omega) - \Sigma_{ph}^{>}(\omega)G^{<}(\omega)]d\omega. \tag{12}$$

We notice that the electron-phonon self-energy (9) is expressed as a linear superposition of individual mode contributions. Inserting Eq. (9) into (12) and exploiting this linearity, it is possible to write the net power emitted in each vibrational mode,

$$W_q = \frac{2}{h}\int_{-\infty}^{+\infty} i_q(\omega)\omega d\omega, \tag{13}$$

where $i_q(\omega)$, given by

$$i_q(\omega) = \mathrm{Tr}[\Sigma_q^{<}(\omega)G^{>}(\omega) - \Sigma_q^{>}(\omega)G^{<}(\omega)], \tag{14}$$

is interpreted as the current at a virtual contact, having the role of breaking the wave function phase and change the electronic energy.[11] Current conservation requires that the net current at the virtual contact must vanish, i.e.,

$$I_q = \int_{-\infty}^{+\infty} i_q(\omega)d\omega = 0. \tag{15}$$

The net rate of phonon emission into the junction required by Eq. (10) can be defined as the ratio between the power dissipated in each mode and the mode energy, $R_q=W_q/\hbar\omega_q$.

The computation of Eq. (13) requires some care in order to avoid numerical inaccuracies. The delicate issue involved in such integration is the necessary condition of current conservation that relays on a cancellation of terms in Eq. (14). In order to fulfill current conservation a rather fine grid becomes necessary, although computationally very expensive. A much better strategy is to split Eq. (14) into the current out-coming (o) and in-coming (i) the virtual contact, respectively, given by the first and the second term of Eq. (14).

Collecting all terms proportional to N_q and N_q+1, each of these contributions can be further divided into absorption (A) and emission (E) components, respectively. Using this procedure, the net current at the virtual contact can be written

$$I_q = \int_{-\infty}^{+\infty} [i^E_{q,o}(\omega) + i^A_{q,o}(\omega) - i^E_{q,i}(\omega) - i^A_{q,i}(\omega)]d\omega, \quad (16)$$

where the emission and absorption terms are

$$i^E_{q,o}(\omega) = (N_q + 1)\mathrm{Tr}[\gamma_q G^<(\omega + \omega_q)\gamma_q G^>(\omega)],$$

$$i^E_{q,i}(\omega) = (N_q + 1)\mathrm{Tr}[\gamma_q G^>(\omega - \omega_q)\gamma_q G^<(\omega)], \quad (17)$$

$$i^A_{q,o}(\omega) = N_q\mathrm{Tr}[\gamma_q G^<(\omega - \omega_q)\gamma_q G^>(\omega)],$$

$$i^A_{q,i}(\omega) = N_q\mathrm{Tr}[\gamma_q G^>(\omega + \omega_q)\gamma_q G^<(\omega)]. \quad (18)$$

Using the invariance of the $\mathrm{Tr}[\cdots]$ under cyclic permutation and changing integration variable it is easy to prove the identities

$$i^E_{q,o}(\omega) = i^E_{q,i}(\omega + \omega_q), \quad (19)$$

$$i^A_{q,o}(\omega) = i^A_{q,i}(\omega - \omega_q). \quad (20)$$

These expressions, inserted back into (13), can be used to show that

$$W_q = \frac{2}{h}\hbar\omega_q \int [i^E_{q,o}(\omega) - i^A_{q,o}(\omega)]d\omega. \quad (21)$$

This final result allows a much easier computation of the emitted power because it does not relay on the subtle cancellation of terms hidden in Eq. (16). Current conservation is guaranteed by construction, as it can be easily shown by inserting the identities (19) and (20) into (16). The result is a numerically reliable expression using a coarser integration grid.

The technical details of our implementation are given in the Appendix. Finally we observe that reduction of this heavy computational step allows one to perform calculations which needs to include the full energetic dependency of the Green's functions, avoiding the simplifying assumptions made in Ref. 5.

Under stationary conditions, Eq. (10) becomes a balance of phonons emitted and dissipated into the contacts. Since R_q itself depends on the number of phonons, a self-consistent loop is necessary in order to find a solution. In order to considerably improve the convergence properties of such a loop, it is better to isolate the linear dependence of R_q on the phonon number N_q as follows:

$$R_q = [(N_q + 1)E_q - N_q A_q], \quad (22)$$

where the explicit form of E_q and A_q can be found from Eq. (21). Oscillatory behaviors and divergences can effectively be removed combining Eqs. (22) with (10), giving an explicit equation for the phonon population at each iteration step of the form

$$N_q = \frac{n_q(T_0)J_q + E_q}{J_q + A_q - E_q}. \quad (23)$$

This expression is particularly instructive, since it allows one to carry several limit results. For instance in the limit of very fast phonon relaxation to the reservoirs ($J_q=\infty$), we find $N_q = n_q(T_0)$. This is an expected result, since it simply means that the coupling is so strong that thermal equilibrium is immediately restored, no matter how fast phonons are emitted in the system. In the opposite limit of no relaxation ($J_q = 0$), phonon absorption by the electrons must balance their emission, leading to

$$N_q = \frac{E_q}{A_q - E_q}. \quad (24)$$

Remarkably, this expression is independent on the electron-phonon coupling γ_q, since E_q and A_q are both proportional to γ_q^2. This can be understood since changes in γ_q modify both the absorption and emission probabilities, leaving the steady state number of phonon, N_q, unchanged.

We also note that a stationary solution is not always guaranteed and generally does not exist whenever $N_q < 0$. From Eq. (25) we get the system stability condition for $J_q + A_q > E_q$. The simple interpretation of this is that $J_q + A_q$ expresses the rate of phonon damping while E_q the rate of phonon creation (it is not actually easy to get a simple interpretation of E_q, since the emission is proportional to N_q+1). Stability is possible only when the damping rate overcomes the emission rate. Whenever these to quantities become close, the steady state number of phonons turns out very large.

Since at steady state the amount of power emitted in the molecule must balance the power dissipated to the reservoirs, a simple (though sometimes not so intuitive) concept can be outlined. For slow dissipations the power emitted is essentially limited by the dissipation rate, J_q. The power emitted must be small and tend to zero as $J_q \to 0$. In the opposite limit of fast dissipation, the power emitted reaches a maximum, only limited by the electron-phonon coupling and by the inelastic tunneling probability, both contained in E_q and A_q.

IV. ANALYTIC MODEL

Explicit expressions for A_q and E_q can be found within the Born approximation and $G^r(E) \approx G^r(E_F)$, $\Sigma^r_{L,R}(E) \approx \Sigma^r_{L,R}(E_F)$. We define $A_{L,R} = G^r\Gamma_{L,R}G^a$ and $T_{\alpha\beta} = \mathrm{Tr}[A^*_\alpha \gamma_q A_\beta \gamma_q]$,

$$E_q = \frac{2}{h}\hbar\omega_q\left[n(\hbar\omega_q)T_{LL} + \left(1 + \frac{eV}{\hbar\omega_q}\right)n(\hbar\omega_q + eV)T_{LR} + \left(1 - \frac{eV}{\hbar\omega_q}\right)n(\hbar\omega_q - eV)T_{RL} + n(\hbar\omega_q)T_{RR}\right], \quad (25)$$

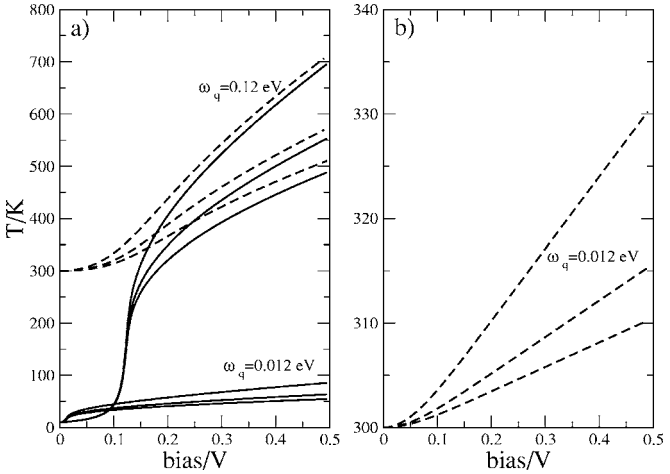

FIG. 1. Molecular temperature vs bias for different parameters. Solid lines are for $T_0=10$ K, dashed lines for $T_0=300$ K. The two groups of three curves correspond to $\omega_q=12$ meV and $\omega_q=120$ meV, $J_q=1\times10^{12}$ Hz, 2×10^{12} Hz, 3×10^{12} Hz, and $T_{LR}=10^{-3}$. Generally T_{mol} decreases as J_q rises.

$$A_q=\frac{2}{h}\hbar\omega_q\Bigg[n(\hbar\omega_q)e^{\beta\hbar\omega_q}(T_{LL}+T_{RR})+\left(1+\frac{eV}{\hbar\omega_q}\right)n(\hbar\omega_q+eV)e^{\beta(\hbar\omega_q+eV)}T_{LR}+\left(1-\frac{eV}{\hbar\omega_q}\right)n(\hbar\omega_q-eV)e^{\beta(\hbar\omega_q-eV)}T_{RL}\Bigg], \quad (26)$$

which is generally valid for all temperatures and biases. The combination of Eq. (23) with (25) and (26) defines the explicit dependence of the nonequilibrium phonon distribution as a function of bias. It is worth noting that the expression $A_q-E_q=\hbar\omega_q\Sigma_{\alpha,\beta}T_{\alpha\beta}$ is a constant, independent of bias (just weakly dependent via $T_{\alpha\beta}$). Once the N_qs are computed, we define the effective molecular temperature, obtained imposing energy conservation,

$$\sum_q \omega_q n_q(T_{mol})=\sum_q \omega_q N_q, \quad (27)$$

where $n_q(T_{mol})$ is the Bose-Einstein distribution with a local temperature T_{mol}, a crucial quantity for the definition of molecular stability.

Based on the analytic equations derived above, we can analyze the dependence of the power dissipated and local temperature in molecular bridges for different choices of the relevant parameters characterizing the junction. In the calculations that follow we assume $T_{LL}=T_{LR}=T_{RL}=T_{RR}$, valid in the case of two identical metallic contacts. For semiconducting contacts $T_{LL}=T_{RR}\approx0$ because backscattering with phonon absorptions is suppressed by the presence of the energy gap. A discussion connecting this terms with phonon decay into electron-hole pairs is given in the Appendix. T_{LR} represent a dimensionless parameter directly related to the phonon emission and absorption rates.

The attention is focused on the molecular temperature as a function of applied bias. In Fig. 1 the local temperature, T_{mol}, is plotted as a function of V for two different choices of the phonon energy (12 and 120 meV). A large sensitivity is found on the crucial parameter J_q and, as expected, higher temperatures are reached for lower J_q. We observe that the local temperature increases for higher mode frequencies and the temperature gradient between contacts and molecule decreases as the reservoir temperature increases. The first mechanism can be understood considering that keeping an identical electron-phonon coupling and dissipation rate, the system reaches the same number of steady state phonons, implying a larger local temperature. The second effect happens because for higher temperatures emission and absorption rates tend to balance, decreasing the net rate of phonon emission. We also observe that in the limit $eV/\hbar\omega_q\gg1$ the molecular temperature becomes linear with bias, whereas the dependence is quadratic for low biases. This behavior can be easily recovered by inspection of Eqs. (25) and (27) which, for large N_q, turns linear in V.

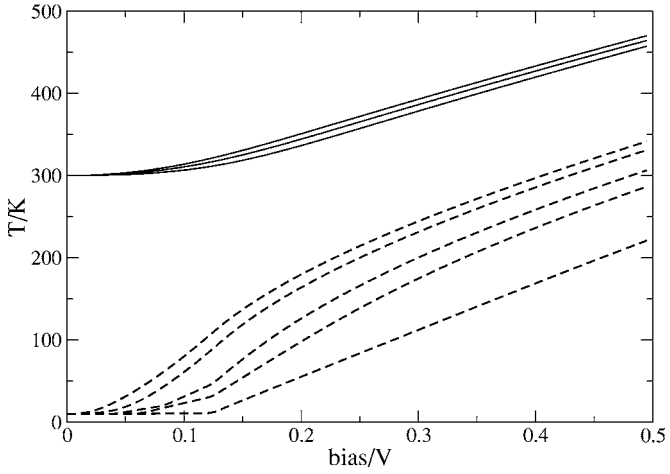

FIG. 2. Molecular temperature vs bias for increasing number of modes uniformly distributed in the range $0<\omega_q<120$ meV, $J_q=1\times10^{12}$ Hz, and $T_{LR}=10^{-3}$.

Figure 1 reveals a sharp increase on the local temperature for biases larger than the mode frequency because emission assisted tunneling take place. When more modes are involved different steps at different characteristic frequencies may be expected, as shown in Fig. 2.

More phenomenological argumentations[27–29] to calculate molecular temperatures under bias are based on the balance between the power emitted, assumed proportional to V^2 as in ohmic conductors, with the power dissipated into the contacts, assumed to behave as σT^4 like in the thermodynamic limit. This leads to a dependence of the junction temperature as $V^{1/2}$. In the present model the balance of power emitted and dissipated is microscopically defined mode by mode through the rate Eq. (10). In the limit of a continuous distribution of modes the power dissipated in the contacts can be written

$$W_{diss}=\sum_q \hbar\omega_q J_q N_q=\int d\omega\rho(\omega)J(\omega)\frac{1}{e^{\beta\hbar\omega}-1}, \quad (28)$$

where $\rho(\omega)$ is the phonon density of states. The density of states of the acoustic phonon bands behaves as $\rho(\omega)=c$ for

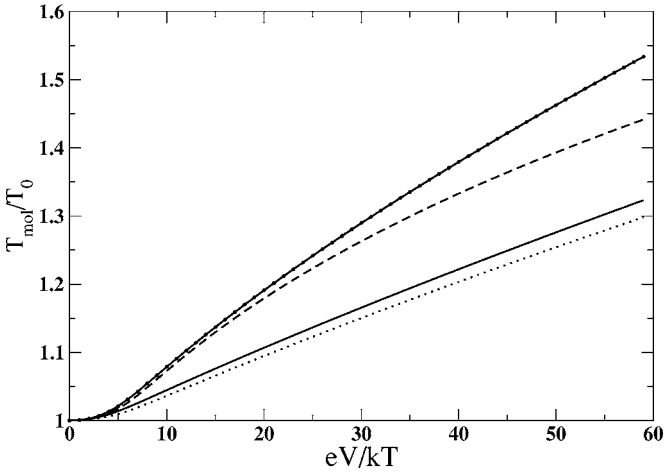

FIG. 3. Molecular temperature vs bias for different distributions of molecular modes. The dashed line corresponds to a distribution $\rho \propto \omega^2$ with a Debeye cutoff $\omega_D=5.74$ kT. The dotted line corresponds to a constant distribution with identical cutoff. The solid lines correspond to one mode only, of energies $\omega_q=\omega_D/2$ (lower) and $\omega_q=2\omega_D/3$ (higher), respectively. The other parameters are $J_q=8\times10^{-5}$ kT/h and $T_{LR}=10^{-7}$.

one-dimensional systems and as $\rho(\omega)=c\omega^2$ for three dimensional systems. Assuming a slow frequency dependent J, in the first case the dissipated power is proportional to T^2, whereas in the second case it is proportional to T^4, recovering the expected behavior of macroscopic systems. On the other hand, the dependence of the power emitted in the molecule, as expressed by $\Sigma_q R_q \hbar\omega_q$, is quadratic in V for low biases but becomes linear for large applied biases, irrespective of the number of vibrational modes or their distribution. This trend, contrasting the ohmic behavior, is an effect of the present model, which assumes that the incoherent current is just a small perturbation of the dominating coherent component and justifying that only one-phonon processes are taken into account. In this regime the power emitted behaves as $\sim\hbar\omega_q I_{inc}\sim\hbar\omega_q V$. In order to recover the ohmic limit, it should be necessary to consider a system much longer than the electron mean free path, such that coherent tunneling is suppressed and propagation is possible only via multiple phonon emissions, releasing all the energy provided by the applied bias. It is worth noting that in the coherent regime the excess energy provided by the bias is released at the collecting contact and is still proportional to V^2 (assuming $I\propto V$).

In light of the discussion above, we deduce that, under the assumption of partially coherent tunneling, the molecular temperature should behave as $T_{mol}\sim V^2$ for low biases turning into $T_{mol}\sim V$ in case that only one or few vibrational modes absorb electron energy. Different trends like $T_{mol}\sim V^{1/2}$ or $T_{mol}\sim V^{1/4}$ are expected when many modes absorb similar amount of energy and their distribution is one-dimensional (first case) or bulklike (second case). These different behaviors are shown in Fig. 3 in terms of dimensionless quantities. The mode distribution assumes a Debye cutoff frequency, $\omega_D=5.74$ kT, which at room temperature corresponds to 1200 cm^{-1}, typical of many molecules.

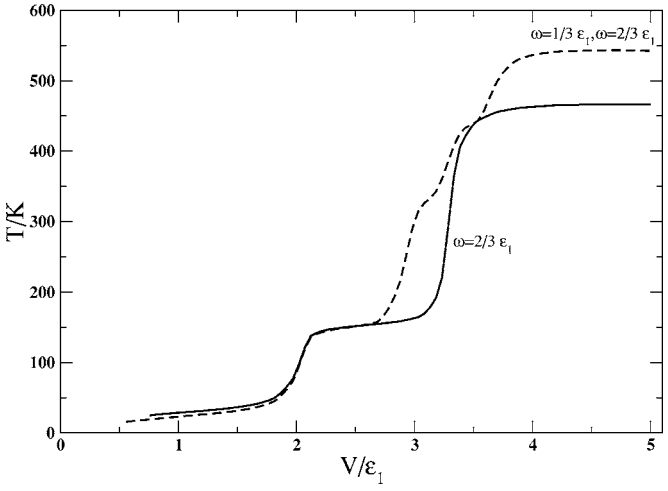

FIG. 4. T_{mol} vs V for a system with a sharp resonating level located at energy ϵ_1 above the Fermi level for $V=0$. The steps correspond to the biases that leads to a sharp enhancement of phonon emission due to assisted tunneling. The solid line is obtained assuming one mode, the dashed line assuming two modes.

V. EFFECT OF RESONANT LEVELS

The results of the previous section are valid in the limit when the energy dependence of the transmission function can be neglected. In this section we show the effect of considering a case where such an assumption cannot be considered valid, such as for instance when a molecular level enters the tunneling energy window. In this case resonant tunneling and phonon assisted emission can take place, changing the qualitative behavior of T_{mol} vs V. The molecular resonance is modeled as a single peak, located off resonance at $V=0$, at an energy ϵ_1 above the Fermi level. Two identical metallic contacts are assumed in this model whose results are shown in Fig. 4. As the bias increases up to $V=2\epsilon_1$ the molecular resonance is brought into the tunneling window (a linear potential drop is assumed) where both coherent and incoherent transport are strongly enhanced, leading to a sharp increase of local temperature. A plateau follows, since the incoherent current levels up. A second rise appears when the bias matches the energy $eV=2(\hbar\omega_q+\epsilon_1)$, corresponding to a second channel for transport assisted by phonon emission.

When more modes are present, more features are expected, as seen in Fig. 4. Clearly for a continuous distribution of modes these features smear out, leaving a broadened step near $V=2\epsilon_1$.

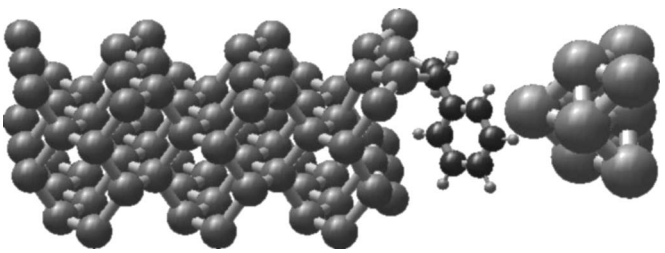

FIG. 5. Figure showing a unit cell of the system with a styrene molecule adsorbed on a Si(100) 2×1. Periodic boundary conditions are imposed on the structure.

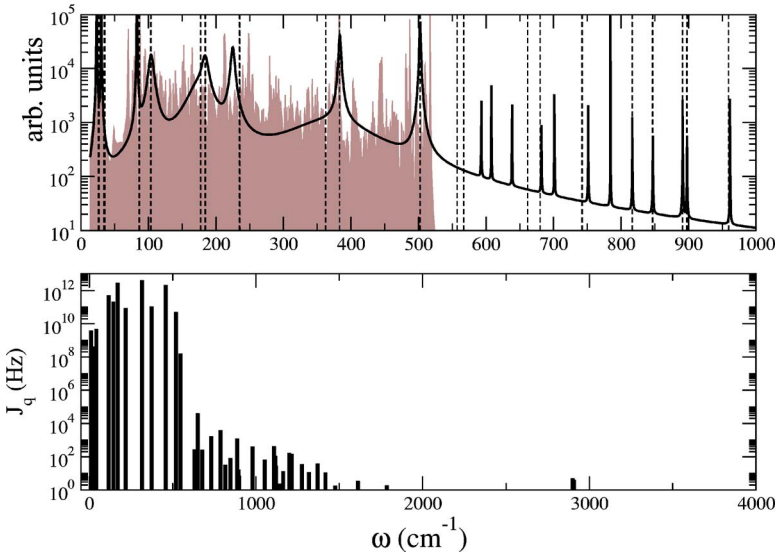

FIG. 6. (Color online) Upper: Phonon DOS of the coupled system Si-substrate+molecule and uncoupled molecular modes (vertical lines). Lower: Phonon decay rates.

This example shows that the electronic density of states can introduce a richness of features in the molecular temperature as a function of bias. From this discussion we have skipped the possibility of semiconducting contacts whose energy gap introduces other characteristic features such as NDR and negative differential heating whenever the tunneling resonances slip below the band edge.

VI. A NUMERICAL SIMULATION

We consider the system shown in Fig. 5, comprising a Si(100) substrate, reconstructed 2×1, with an adsorbed styrene molecule in a bridge position and an Ag metal contact which could model an STM tip. The position of the tip was chosen in order to obtain a relatively large direct coupling between the tip and the π orbitals of the styrene which guarantees a sufficiently high conductance. The figure shows a unit cell of the system considered, but periodic boundary conditions are imposed.

The Si substrate is heavily p doped in order to make it conducting and the Fermi level is assumed at the valence band edge. While electrons cross the molecule, they interact with the molecular ionic vibrations from which they can be inelastically scattered. The electron-phonon scattering within the leads is not considered in this work.

In order to study the electron-vibron coupling we first relax very accurately the structure (this is done under no applied bias). Then we compute the vibrations of the molecule constraining the Si and Ag atoms. The calculation is then repeated allowing all atoms to be free to move. This calculation allows one to compute the coupling of the molecular modes with the Si substrate and to compute the decay rate of such vibrations into the contacts.

This type of first-principles calculation applied to phonon decay is presented here for the first time to our knowledge. The result of such a calculation is shown in Fig. 6, reporting in the upper panel the superposition of the phonon density of states of the coupled system with the uncoupled molecular frequencies shown as vertical dashed lines. The phonon density of states (DOS) of the Si substrate is shown as a gray area where the cutoff frequency of 500 cm^{-1} is clearly visible. The modes within the Si bandwidth show a sizeable broadening due to the interaction with the contacts. As the frequency rises above the cutoff both broadening and frequency shift become very small. The lower panel of Fig. 6 reports the decay rates, J_q, computed from the broadening of each molecular mode. The model gives realistic results for those molecular modes lying within the Si phonon bands, however, they decrease fast as the molecular frequencies go beyond this band. On the light of the discussion made in Sec. III, decay rates as slow as 10^2 Hz are rather unrealistic, therefore the lowest limit of decay of 10^6 Hz has been fixed in subsequent calculations.

We find that the out of equilibrium phonon population is strongly bias dependent. At the applied bias of 0.95 V, a molecular resonance (shown in Fig. 9) enters the injection window, with the effect of strongly increasing the coherent and incoherent currents. On average all vibrational modes are excited as the bias increases, although some of them are particularly favored, such as the lowest vibrational mode. This depends on the electron-phonon couplings shown in

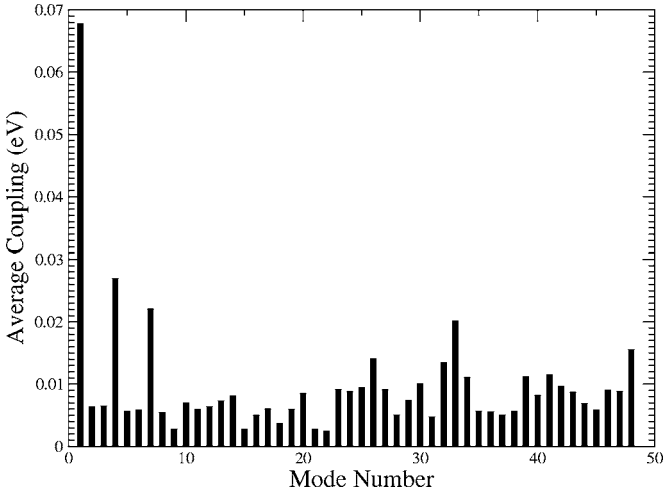

FIG. 7. Average electron-phonon coupling for each mode.

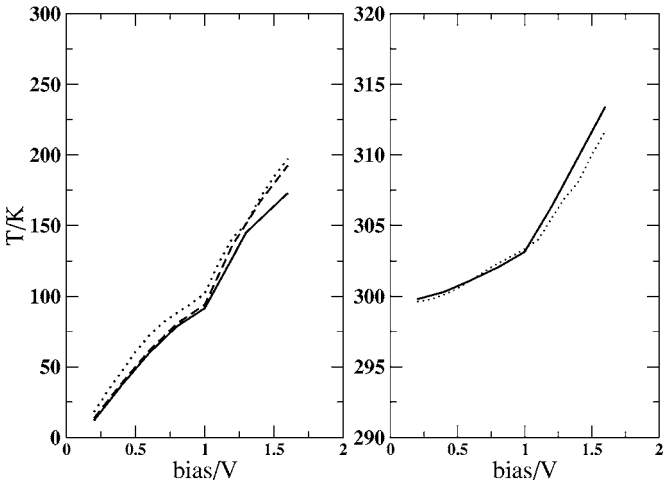

FIG. 8. Molecular temperature as a function of bias for different contact temperatures. Left, $T_0=0$. Right, $T_0=300$ K. Dotted, dashed, and solid lines correspond, respectively, to lowest order, BA, and SCBA.

Fig. 7. First we project the electron-phonon coupling matrices, M_q, on the molecular orbitals, ψ_i, by computing the matrix elements $\langle\psi_i|M_q|\psi_i\rangle$. Since the tunneling process occurs via the molecular orbitals (MO) resonances, these matrix elements give an indication about which modes have larger *el-ph* interactions. We observe that the lowest mode dominates over most molecular orbitals, and gives the largest average coupling. The lowest vibrational mode, at the frequency of 10.55 cm^{-1}, corresponds to a rigid oscillation of the whole benzene ring, away and toward the Ag tip, leading to a strong variation of the molecule-metal matrix elements and, therefore, to a large electron-phonon coupling. This explains why the phonon emission mostly occurs into the lowest energy mode, once the first resonant tunneling is hit.

Figure 8 reports the behavior of the molecular temperature as a function of applied bias for two different contact temperatures. It is possible to appreciate the change in slope at the applied bias of 1.0 V. The figure reports three different calculations obtained for the simplest lowest order calculation, not including the electron-phonon self-energy renormalization of the electron propagator, the first order correction, commonly known as first order Born approximation (BA) and the self-consistent Born approximation (SCBA). Because of the small incoherent tunneling current, the inclusion of higher orders bring only small corrections to the final result.

The computed current density within the bias window at 2.0 V is shown in Fig. 9, where it is possible to see the resonance peak at −5.25 eV. The figure shows the total current and the coherent component. The incoherent component (not shown) is about two orders of magnitude smaller, except at the resonance, where it becomes comparable. The total tunneling current computed at 1.0 V is 1.2 nA.

The molecular temperature sensibly depends on the tunneling current, which can be changed by varying the tip-molecule distance. When this distance becomes approximately 2.0 Å the flowing current reaches 0.5 μA, leading to a very large temperature increase ($\approx$1000 K). Obviously the molecule is not likely to withstand such temperatures and may rather desorb.

VII. CONCLUSIONS

Several aspects of heat dissipation in a molecular bridge has been touched on in this paper. Useful identities have been derived, allowing a stable computation of the phonon emission rate in the junction which avoids computationally heavy integration grids. The self-consistent loop used to compute the steady state phonon population of the junction have been linearized and solved in an explicit way in order to avoid divergences and oscillatory behaviors. Several trends of molecular temperature vs bias have been discussed under different scenarios with the help of both analytic results and numerical calculations. We find that local temperature sensibly depends on the dissipation rate of the phonon into the bath and the inelastic transmission probability, containing both electron-phonon coupling and density of states information. Tunnelling resonances introduce a reach "spectroscopy" that could be revealed in future measurements. Finally our

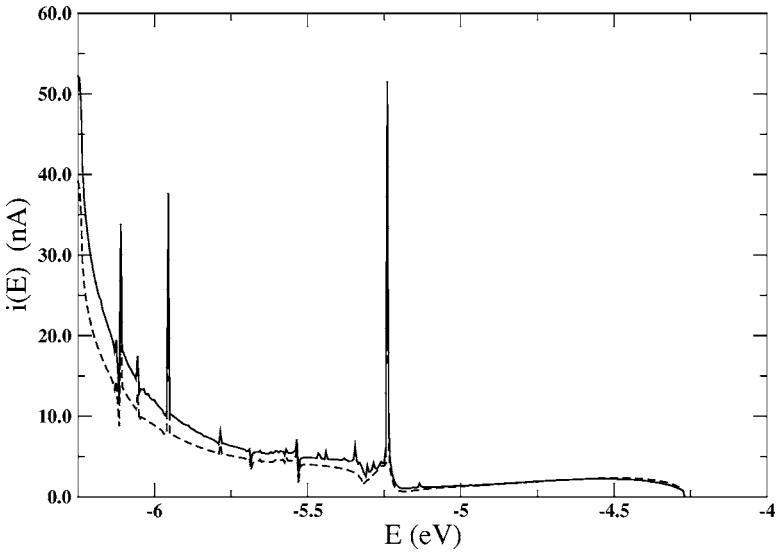

FIG. 9. Total and coherent component of the current density in the energy window relevant for integration.

model has been applied to a realistic system comprising a styrene molecule adsorbed on a Si substrate and a weakly coupled metal contact. The calculation is completely obtained from first-principles calculations, including structure relaxation, vibrational frequencies, electron-phonon couplings, and phonon decay rates into the contacts. We find that after the critical voltage of 1.0 V the lowest vibrational mode of free oscillations of the styrene molecule becomes strongly excited, and the molecular temperature sharply rises above this voltage. Junction stability sensibly depends on the tunneling current and the bonding to the substrate is likely to be unstable for tip-molecule distances smaller than 2.5 Å.

APPENDIX A

The numerical simulator implements two nested self-consistent loops. The innermost loop solves the SCBA, which requires the iterative calculations of several equations. We start by assuming that the initial phonon self-energy is zero, $\Sigma_0^{<,>}=0$, then we define the contact self-energies, which are stored on disk and reused at each iterations, since they do not change,

$$\Sigma_n^{<(>)}(\omega)=\Sigma_L^{<(>)}(\omega)+\Sigma_R^{<(>)}(\omega)+\Sigma_{ph,n}^{<(>)}(\omega). \quad \text{(A1)}$$

Then define the imaginary part of the electron-phonon self-energy,

$$\Sigma_{ph,n}^{r}(\omega)=\frac{1}{2}[\Sigma_{ph,n}^{>}(\omega)-\Sigma_{ph,n}^{<}(\omega)], \quad \text{(A2)}$$

and the total self-energy,

$$\Sigma_n^r(\omega)=\Sigma_L^r(\omega)+\Sigma_R^r(\omega)+\Sigma_{ph,n}^r(\omega). \quad \text{(A3)}$$

This enables the computation of the system Green's function,

$$G_n^r(\omega)=[\omega S-H-\Sigma_n^r(\omega)]^{-1}. \quad \text{(A4)}$$

The correlation function is then solved from the kinetic equation,

$$G_n^{<(>)}(\omega)=G_n^r(\omega)\Sigma_n^{<(>)}(\omega)G_n^a(\omega). \quad \text{(A5)}$$

Finally, the electron-phonon scattering can be computed from

$$\Sigma_{ph,n+1}^{<,>}=N_q\gamma_q G_n^{<,>}(E\mp\omega_q)\gamma_q+(N_q+1)\gamma_q G_n^{<,>}(E\pm\omega_q)\gamma_q. \quad \text{(A6)}$$

Equations (A2)–(A6) are iterated for $n=0,1,\ldots,\infty$. The loop can be stopped at any step and $G_n^{<(>)}(\omega)$, $\Sigma_{ph,n+1}^{<(>)}(\omega)$ can be used to compute the phonon emission rate and current. It may be observed that this scheme ensures current conservation since $\Sigma_{ph}^{<,>}$ are computed from the same $G^{<,>}$ used in (14) to compute the virtual contact current and the emitted power (12). This trick can be used in programming efficiently a SCBA loop which guarantees a correct calculation of the emitted power even when stopped after the first or a few steps. It is worth noting that when the loop is stopped at the second iteration ($n=1$) the virtual contact current already contains terms of second order, whereas the current through the molecule is accurate to first order approximation. In general the power emitted is accurate to order $n+1$, and the current flowing through the molecule is accurate to order n. In this way the virtual contact current is guaranteed to vanish for any n, giving a correct result for the emitter power and rate of phonon emission. The inconsistence disappears in the SCBA, but it is not of great concern, since the calculation of phonon emission rate and current can be considered independent.

APPENDIX B

In this appendix we discuss the mechanism of phonon damping into electron-hole pairs, the most important phonon decay channel for molecules adsorbed on metallic contacts. We point out that the computation of such decay is accounted for within the net emission rate, R_q, computed using (13). This is a quite relevant observation for efficient calculations because it spares the computation of the phonon self-energy from the polarization diagram, that should be calculated as the convolution

$$\Pi_q^{<,>}(\omega)=-\frac{i}{2\pi}\int \gamma_q G^{<,>}(\omega')\gamma_q G^{>,<}(\omega'-\omega)d\omega'. \quad \text{(B1)}$$

The phonon decay rate can be expressed as

$$\frac{1}{\tau_q}=-\frac{2}{\hbar}\,\mathrm{Im}\{\mathrm{Tr}[\Pi_q^r(\omega_q)]\}=-\frac{1}{\hbar}\mathrm{Tr}[\Pi_q^{>}-\Pi_q^{<}]. \quad \text{(B2)}$$

By developing to lowest order Eq. (B1) we get

$$G^{<}(\omega)=if_\alpha(\omega)A_\alpha(\omega)\approx if_\alpha(\omega)A_\alpha(E_F) \quad \text{(B3)}$$

which implies, after lengthy integrations,

$$\frac{1}{\tau_q}=\frac{2\hbar\omega_q}{h}\mathrm{Tr}[\gamma_q A(E_F)\gamma_q A(E_F)]. \quad \text{(B4)}$$

In the above expression we have defined the total spectral function as $A(E)=\Sigma_k A_k(E)$. Because of the Fermi functions the integrations give a contribution only close to the electrochemical potentials of the two contacts. This term includes all mechanisms of phonon absorptions, both as a result of tunneling from one contact to the other as well as reflections at the two molecular interfaces. Such reflections can be also recovered when computing the rate of phonon absorption using the virtual contact current, corresponding to real generations of electron-hole pairs that are assumed to recombine within the charge reservoirs.

[1] Z. Huang, B. Xu, Y. Chen, M. Di Ventra, and N. J. Tao, Nano Lett. **6**, 1240 (2006).
[2] T. N. Todorov, J. Hoekstra, and A. P. Sutton, Phys. Rev. Lett. **86**, 3606 (2001).
[3] Y. C. Chen and M. Di Ventra, Phys. Rev. Lett. **95**, 166802 (2005).
[4] A. Pecchia, A. Gagliardi, S. Sanna, T. Frauenheim, and A. Di Carlo, Nano Lett. **4**, 2109 (2004).
[5] M. Paulsson, T. Frederiksen, and M. Brandbyge, Phys. Rev. B **72**, 201101(R) (2005).
[6] D. Segal and A. Nitzan, J. Chem. Phys. **117**, 3915 (2002).
[7] M. Elstner, D. Porezag, G. Jungnickel, J. Elsner, M. Haugk, T. Frauenheim, S. Suhai, and G. Seifert, Phys. Rev. B **58**, 7260 (1998).
[8] D. Porezag, T. Frauenheim, T. Kohler, G. Seifert, and R. Kaschner, Phys. Rev. B **51**, 12947 (1995).
[9] T. Frauenheim, G. Seifert, M. Elstner, Z. Hajnal, G. Jungnickel, D. Porezag, S. Suhai, and R. Scholz, Phys. Status Solidi B **271**, 41 (2000).
[10] A. Di Carlo, Physica B **314**, 211 (2002).
[11] A. Pecchia and A. Di Carlo, Rep. Prog. Phys. **67**, 1497 (2004).
[12] D. Porezag, M. R. Pederson, T. Frauenheim, and T. Köhler, Phys. Rev. B **52**, 14963 (1995).
[13] G. Seifert, D. Porezag, and T. Frauenheim, Int. J. Quantum Chem. **98**, 185 (1996).
[14] N. Mingo and K. Makoshi, Phys. Rev. Lett. **84**, 3694 (2000).
[15] E. G. Emberly and G. Kirczenow, Phys. Rev. B **61**, 5740 (2000).
[16] H. Ness and A. J. Fisher, Chem. Phys. **281**, 279 (2002).
[17] B. Dong, H. L. Cui, and X. L. Lei, Phys. Rev. B **69**, 205315 (2004).
[18] Y. Meir and N. S. Wingreen, Phys. Rev. Lett. **68**, 2512 (1992).
[19] L. V. Keldysh, Sov. Phys. JETP **20**, 1018 (1965).
[20] L. P. Kadanoff and G. Baym, *Quantum Statistical Mechanics* (W. A. Benjamin, New York, 1962).
[21] M. Galperin, M. Ratner, and A. Nitzan, Nano Lett. **4**, 1605 (2004).
[22] A. Nitzan, S. Mukamel, and J. Jortner, J. Chem. Phys. **60**, 3929 (1973).
[23] M. Budde, G. Lupke, C. P. Cheney, N. H. Tolk, and L. C. Feldman, Phys. Rev. Lett. **85**, 1452 (2000).
[24] A. Nitzan, *Chemical Dynamics in Condensed Phases* (Oxford University Press, Oxford, 2006).
[25] A. Pecchia, G. Romano, and A. Di Carlo (unpublished).
[26] S. Datta, *Electronic Transport in Mesoscopic Systems* (Cambridge University Press, Cambridge, 1995).
[27] Y. C. Chen, M. Zwolak, and M. Di Ventra, Nano Lett. **3**, 1691 (2003).
[28] Y. C. Chen, M. Zwolak, and M. Di Ventra, Nano Lett. **5**, 621 (2005).
[29] T. N. Todorov, J. Hoekstra, and A. P. Sutton, Phys. Rev. Lett. **86**, 3606 (2001).